ORGANOMETALLICS

Article

Cite This: *Organometallics* 2019, 38, 2523−2529

pubs.acs.org/Organometallics

Unravelling the Photochemical Transformations of Chromium(I) 1,3 Bis(diphenylphosphino), $[Cr(CO)_4(dppp)]^+$, by EPR Spectroscopy

Stephen L. J. Luckham,[†,‡] Andrea Folli,*[,†] James A. Platts,[†] Emma Richards,*[,†] and Damien M. Murphy*[,†]

[†]School of Chemistry, Cardiff University, Main Building, Park Place, Cardiff CF10 3AT, U.K.

[‡]School of Chemistry, University of Bristol, Cantock's Close, Bristol BS8 1TS, U.K.

Supporting Information

ABSTRACT: UV-induced photochemical transformations of the paramagnetic $[Cr(CO)_4(Ph_2PCH_2CH_2CH_2PPh_2)]^+$ complex (abbreviated $[Cr(CO)_4(dppp)]^+$) in dichloromethane was investigated by CW EPR spectroscopy. Room-temperature UV irradiation results in the rapid transformation of $[Cr(CO)_4(dppp)]^+$ into *trans*-$[Cr(CO)_2(dppp)_2]^+$. However, low-temperature (77−120 K) UV irradiation reveals the presence of an intermediate *mer*-$[Cr(CO)_3(\kappa^1\text{-dppp})(\kappa^2\text{-dppp})]^+$ complex which photochemically transforms into *trans*-$[Cr(CO)_2(dppp)_2]^+$. The derived spin Hamiltonian parameters for these complexes were confirmed by DFT calculations. The photoinduced reaction is shown to be concentration-dependent, leading to a distribution of the three complexes ($[Cr(CO)_4(dppp)]^+$, *mer*-$[Cr(CO)_3(\kappa^1\text{-dppp})(\kappa^2\text{-dppp})]^+$, and *trans*-$[Cr(CO)_2(dppp)_2]^+$). A bimolecular photoinduced mechanism is proposed to account for the formation of *mer*-$[Cr(CO)_3(\kappa^1\text{-dppp})(\kappa^2\text{-dppp})]^+$ and *trans*-$[Cr(CO)_2(dppp)_2]^+$.

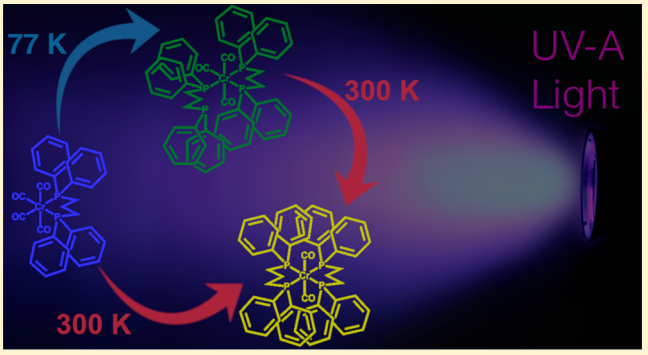

INTRODUCTION

Cr-based complexes are important catalysts for the selective trimerization/tetramerization of ethylene to yield highly desirable linear α-olefins.[1−7] These catalysts typically employ ligands based on bis(phosphino)amines and bis(sulfanyl)-amines, whereby the activity and selectivity of the catalytic reactions can in principle be tuned by varying the nature of the ancillary ligands.[5] Since the first reports of ethylene tetramerization toward 1-octene using chromium-bis-(diphenylphosphino)amine (Cr-PNP) catalysts, many studies have focused on the mechanism, with particular reference to the oxidation states of the active chromium centers. In most cases, these Cr-based complexes are generally activated prior to catalysis by addition of an alkylaluminum cocatalyst, such as triethylaluminum (Et_3Al) or methylaluminoxane (MAO).[5]

While electron paramagnetic resonance (EPR) studies have been used to study the oxidation states of chromium following the activation step,[7,8] previous work from our group revealed the important role that the ligand itself plays in adopting various conformations of the partially or fully decarbonylated complexes.[9−11] For example, addition of triethylaluminum (Et_3Al) in nonaromatic solvents to $[Cr(CO)_4(Ph_2P(C_2H_4)PPh_2)]^+$ (1,2-bis(diphenylphosphino)ethane, $Ph_2P(C_2H_4)PPh_2$ = dppe) or $[Cr(CO)_4(Ph_2PN(i\text{Pr})PPh_2)]^+$ (1,2-bis-(diphenylphosphino)-isopropylamine, $Ph_2PN(i\text{Pr})PPh_2$) resulted in the formation of the Cr(I)-bis-η^6-arene complex, formed via intramolecular rearrangement and coordination of Cr(I) to the phenyl groups of the bis(diphenylphosphino) ligand.[10] Several additional complexes, including *cis*-$[Cr(CO)_3(Ph_2PN(i\text{Pr})PPh_2)]^+$ and the piano-stool type $[Cr(CO)_2(Ph_2PN(i\text{Pr})PPh_2)]^+$ complexes, were also identified following Et_3Al activation of $[Cr(CO)_4(Ph_2PN(i\text{Pr})PPh_2)]^+$, revealing the structural rearrangements that occur in these complexes.[11]

Despite the widely studied chemistry of these tetracarbonyl chromium-bis(diphenylphosphino)amine complexes, particularly from the perspective of catalysis, what remains sparsely studied to date is the photochemistry of these Cr(I) systems. The photochemistry, photophysics, and photoelectrochemistry of metal carbonyl complexes have, in general, been studied extensively over the years,[12−15] and for example, the loss of a carbonyl ligand from $Cr(CO)_6$ is one of the fastest photochemically induced processes known, occurring on a femtosecond time scale.[12] With respect to Cr(0) tetracarbonyl complexes, Perutz et al. performed very detailed transient absorption studies on the phototransformations of the (bis(bis(penta-fluoroethyl)phosphino)ethane) tetracarbonyl chromium complex.[15] Photoactivation of Cr(I) complexes by UV was also observed by researchers at SASOL, using the same alkylaluminum cocatalyst as used here.[16] Interestingly, they also observed (via IR) the reformation of the Cr(0)

Received: April 3, 2019
Published: June 13, 2019

DOI: 10.1021/acs.organomet.9b00226
Organometallics 2019, 38, 2523−2529

complex following UV irradiation, accounting for the observed loss of Cr(I) centers.[16] By comparison, the photochemistry of Cr(I) complexes with *fac*- and *mer*-$[Cr(CO)_3(\kappa^1\text{-}L_2)(\kappa^2\text{-}L_2)]^+$ (L_2 = bidentate phosphine, abbreviated as dppe) coordination has been less widely investigated by EPR.[17] The facial complex was shown to rapidly isomerize to the meridional structure via a thermally activated process. The *mer*-complex was then found to lose CO in a photochemical UV-driven transformation to produce the *trans*-$[Cr(CO)_2(L_2)_2]^+$ complex. However, the *fac*- and *mer*-$[Cr(CO)_3(\kappa^1\text{-dppe})(\kappa^2\text{-dppe})]$ Cr(0) complexes were initially synthesized and isolated, before one-electron oxidation of the *mer*-complex by $[Fe(\eta\text{-}C_5H_5)_2]^+$ or $[O_2NC_6H_4N_2]^+$ to give the corresponding Cr(I) species.[17] To date, the photochemistry and UV-induced decarbonylation of the paramagnetic $[Cr(CO)_4(Ph_2P(C_3H_6)PPh_2)]^+$ (1,3 bis(diphenylphosphino)propane, $Ph_2P(C_3H_6)PPh_2$ = dppp), have never been investigated. Therefore, using EPR and DFT, herein we explore for the first time the photochemical transformations of the tetracarbonyl Cr(I) system, $[Cr(CO)_4(dppp)]^+$ (Scheme 1) and examine the underlying photoinduced mechanism.

Scheme 1. Structure of the Chromium(I) 1,3 Bis(diphenylphosphino) Complex Investigated Herein (Labeled $[Cr(CO)_4(dppp)]^+$) and the Associated Counterion

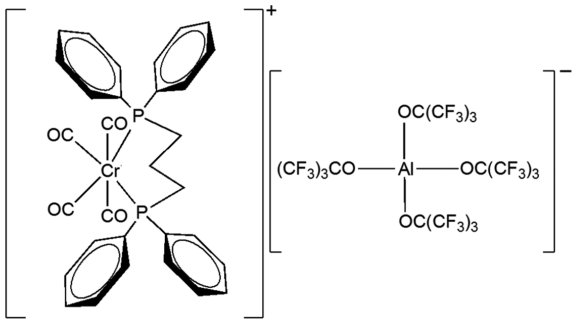

RESULTS AND DISCUSSION

The 140 K CW EPR spectrum of $[Cr(CO)_4(dppp)]^+$ (compound **1**) in frozen solution is shown in Figure 1a. This EPR spectrum, previously discussed in detail by us for a series of analogous Cr(I) complexes,[8] is characterized by an axial **g** tensor ($g_\perp > g_e > g_\parallel$) with a large hyperfine coupling characterized by a 1:2:1 multiplet pattern, originating from the interaction of the unpaired electron with two equivalent ^{31}P (I = 1/2) nuclei (Table 1). The spin Hamiltonian parameters, obtained by simulation of the experimental spectra, were shown to be consistent with a low-spin d^5 Cr(I) center possessing a SOMO of largely d_{xy} character. The corresponding fluid solution (i.e., isotropic) EPR spectrum produces a broad, structureless signal due to fast relaxation characteristics. The simulated spin Hamiltonian parameters are in good agreement with the parameters obtained by DFT for the geometry optimized structure (Figure 2).

Following UV irradiation of the $[Cr(CO)_4(dppp)]^+$ complex at 298 K (after ca. 30 min), the intense blue coloration of the solution changed to pale yellow and this was accompanied by a significant change to the anisotropic EPR spectrum (Figure 1b). A new EPR spectrum can be identified by a characteristic

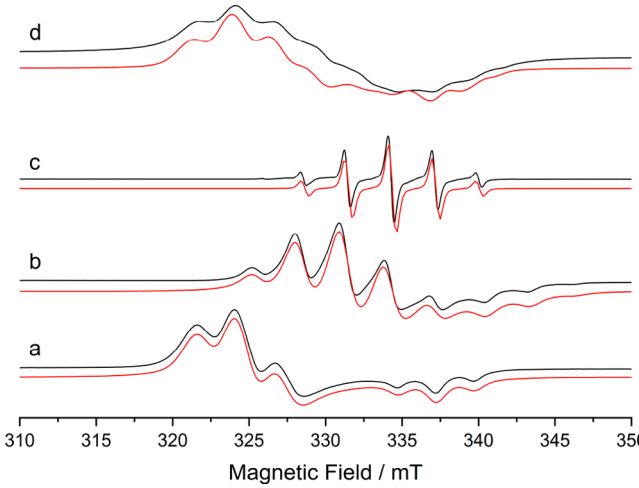

Figure 1. X-band CW EPR spectra of (a) $[Cr(CO)_4(dppp)]^+$, (9.7 mM) recorded at 140 K and (b,c) $[Cr(CO)_2(dppp)_2]^+$ formed by UV irradiation of $[Cr(CO)_4(dppp)]^+$ at 298 K and recorded at (b) 140 K and (c) 298 K, respectively. The EPR spectrum of a mixture of the starting complex (40% spectral contribution) and *mer*-$[Cr(CO)_3(\kappa^1\text{-dppp})(\kappa^2\text{-dppp})]^+$ (60% spectral contribution) formed by UV irradiation of $[Cr(CO)_4(dppp)]^+$ at 77 K is also shown in (d). The corresponding simulations are shown in red (parameters given in Table 1).

axial g and ^PA profile with $g_\perp$ = 2.024 and $g_\parallel$ = 1.968, possessing a notably smaller g anisotropy compared to the starting $[Cr(CO)_4(dppp)]^+$ complex (Table 1). Changes to the multiplicity of the ^{31}P superhyperfine coupling, which is superimposed on both the parallel and perpendicular components of the signal, are also clearly observed. This indicates the formation of a new Cr(I) complex. The distinctive 5-line multiplet pattern (with relative intensities of 1:4:6:4:1) is more readily resolved in the isotropic EPR spectrum (Figure 1c) because of coupling of the unpaired electron with four equivalent ^{31}P nuclei. At high resolution, weak ^{53}Cr satellite features are also observed in the wings of this isotropic spectrum (see Figure S13), confirming the origin of the signal to a Cr(I) center. Simulation of the anisotropic and isotropic EPR spectra for this new complex revealed the ^PA coupling components to be a_{iso} = −81.3 MHz, $A_\perp$ = −82 MHz, and $A_\parallel$ = −80 MHz. The negative sign of the superhyperfine couplings is chosen to be compatible with the DFT-calculated values, which predict a negative spin density at the phosphorus atom. There is indeed negative spin density on the P atoms: Mulliken spin density on coordinated P is consistently around −0.03 to −0.04 e. We attribute this to mixing of metal d-orbitals with ligand-based ones in the less-than-octahedral symmetry of these complexes, which is also evident in Mayer bond orders for Cr−P of approximately 0.5. The ^{31}P superhyperfine tensor orientations (and matrices) are shown in the SI, along with a summary table of the spin Hamiltonian parameters for a general series of Cr(I) complexes.

The new Cr(I) complex identified in Figure 1b,c must arise from a partially decarbonylated complex in which two equivalents of the dppp ligand are now directly coordinated to the chromium metal center in a *trans*- conformation, hereafter labeled *trans*-$[Cr(CO)_2(dppp)_2]^+$ (compound **2**). The spin Hamiltonian parameters for this *trans*-$[Cr(CO)_2(dppp)_2]^+$ complex, obtained by simulation of the spectra, are in good agreement with the DFT derived values

DOI: 10.1021/acs.organomet.9b00226
Organometallics 2019, 38, 2523−2529

Table 1. Spin Hamiltonian Parameters for the Three Paramagnetic Cr(I) Complexes, $[Cr(CO)_4(dppp)]^+$ (1), *trans*-$[Cr(CO)_2(dppp)_2]^+$ (2) and *mer*-$[Cr(CO)_3(\kappa^1\text{-dppp})(\kappa^2\text{-dppp})]^+$ (3)[a]

					α	β	γ				α	β	γ
					Euler angles rotation of the g frame with respect to the molecular frame						Euler angles rotation of the *A* frame with respect to the molecular frame		
compound		g_1	g_2	g_3	/deg	/deg	/deg	$^{31P}A_1$ /MHz	$^{31P}A_2$ /MHz	$^{31P}A_3$ /MHz	/deg	/deg	/deg
1	expt	1.988	2.066	2.066	−180	90	60	−65	−77	−77	−120	160	120
								−65	−77	−77	−60	160	60
	DFT	1.992	2.029	2.039	−188	99	66	−68	−70	−78	−115	156	110
								−64	−66	−74	−61	165	83
2	expt	1.968	2.024	2.024	90	120	180	−80	−82	−82	−20	120	45
								−80	−82	−82	20	120	120
								−80	−82	−82	−20	120	45
								−80	−82	−82	20	120	120
	DFT	1.964	2.009	2.012	90	117	180	−80	−81	−92	−23	125	41
								−80	−81	−92	23	125	139
								−80	−81	−92	−23	125	41
								−80	−81	−92	157	55	−41
3	expt	1.984	2.026	2.050	15	60	180	−44	−50	−60	−120	90	−60
								−70	−70	−83	0	90	60
								−44	−50	−60	90	60	−180
	DFT	1.982	2.014	2.024	14	64	172	−43	−47	−60	−120	85	−68
								-0.4	*-0.5*	*-0.5*	*53*	*54*	*133*
								−70	−70	−83	−3	105	53
								−44	−51	−58	83	55	−180

[a]Uncertainties of the experimental spin Hamiltonian parameters are ±0.003 for the g-values and ±3 MHz for the super-hyperfine couplings. Euler angles are provided in degrees with uncertainties of ±10 deg. In the *mer*-$[Cr(CO)_3(\kappa^1\text{-dppp})(\kappa^2\text{-dppp})]^+$ (**3**) complex, the theoretical hyperfine couplings to the second ^{31}P on the κ^1-dppp ligand, which is not directly binding to the Cr center, are shown in italics and they could not be measured experimentally by CW EPR (vide infra).

(Table 1). The observed parameters are also analogous to those previously reported in the literature for structurally similar complexes,[17−21] but in those cases, the complexes were typically formed via chemical or electrochemical oxidation of the Cr(0) *mer*-$[Cr(CO)_3(\kappa^1\text{-}L_2)\ (\kappa^2\text{-}L_2)]^0$ (L_2 = bidentate phosphine) structures yielding the paramagnetic Cr(I) system which then slowly decays to the *trans*-$[Cr(CO)_2(L_2)_2]^+$ complex (Table 1). In the current work, the EPR spectrum of *trans*-$[Cr(CO)_2(dppp)_2]^+$ (Figure 1b,c) remained unchanged following storage in the dark at 298 K for 48 h, indicating that this complex is kinetically inert. The equivalency of the ^{31}P hyperfine couplings in the spectra (Figure 1b,c) also clearly indicate the formation of the *trans* -isomer, as opposed to the *cis*- isomer, in agreement with the known preference for stabilization of *trans*- complexes over the corresponding *cis*-Cr(I) complexes.[22]

Formation of the *trans*-$[Cr(CO)_2(dppp)_2]^+$ complex, starting only from $[Cr(CO)_4(dppp)]^+$, clearly requires the presence of two dppp ligands for every Cr(I) center. Considering no excess ligand was present in the studied system, this implies that 2 equiv of the starting $[Cr(CO)_4(dppp)]^+$ complex are required for formation of 1 equiv of *trans*-$[Cr(CO)_2(dppp)_2]^+$. Interestingly, the formation of *trans*-$[Cr(CO)_2(dppp)_2]^+$ (Figure 1b) is accompanied by a considerable loss of EPR signal intensity. One possible explanation is that $[Cr(CO)_6]^+$ is formed during the photochemical transformation of $[Cr(CO)_4(dppp)]^+$ into *trans*-$[Cr(CO)_2(dppp)_2]^+$ or that phosphine-free Cr(I) ions are released into solution and not observed by EPR. Although the EPR spectrum of $[Cr(CO)_6]^+$ has only once been reportedly observed at 4 K,[23] Bond et al. gave a very comprehensive explanation on the failure to observe isotropic EPR signals for such a species.[24] Therefore, if $[Cr(CO)_6]^+$ is indeed formed, it would prove exceedingly difficult to detect by conventional X-band EPR. All attempts to detect $[Cr(CO)_6]^+$ in our experiments by EPR, and additionally by chemical oxidation of $[Cr(CO)_6]$ with $Ag[Al(OC(CF_3)_3)_4]$, proved to be unsuccessful, even at low temperatures (5 K). However, there is previous EPR evidence for this $17e^-$ complex which was described as having a single broad line,[23] while Pickett and Pletcher[25] noted that disproportionation of the cation can occur yielding an unstable $[Cr(CO)_6]^{2+}$ complex and reformation of the starting $[Cr(CO)_6]$. Evidence for the release of phosphine-free Cr(I) into solution was also explored here through the addition of toluene to the solvent mixture. In previous work by our group, chemical activation of $[Cr(CO)_4(dppp)]^+$ resulted in the formation of a bis-toluene complex $[Cr(\eta^6\text{-}(CH_3)C_6H_5)_2]^+$ in aromatic solvents.[9,10] Therefore, if free Cr(I) ions were released during the UV irradiation, it might reasonably be expected that a signal for $[Cr(\eta^6\text{-}(CH_3)C_6H_5)_2]^+$ could be detected; however no evidence for this signal was observed following UV irradiation in the presence of toluene.

To better understand the mechanism of *trans*-$[Cr(CO)_2(dppp)_2]^+$ formation, the UV photolysis experiments of $[Cr(CO)_4(dppp)]^+$ were conducted at low temperatures (77 K). A typical EPR spectrum obtained under these low-temperature conditions is shown in Figure 1d. UV irradiation at 77 K for up to 120 min led to a marked color change in the solution, from intense blue to green, resulting in the accompanying new signal shown in Figure 1d. Despite the broad line widths, it can clearly be seen that the profile of this

DOI: 10.1021/acs.organomet.9b00226
Organometallics 2019, 38, 2523−2529

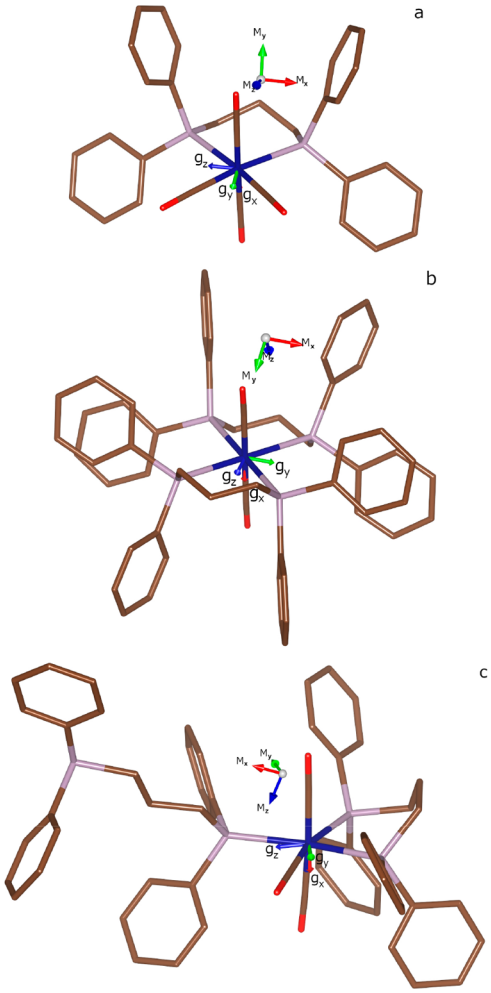

Figure 2. Geometry-optimized structures of the paramagnetic Cr(I) complexes at the uBP86/def2-TZVP level of theory. Structures include (a) $[Cr(CO)_4(Ph_2PCH_2CH_2CH_2PPh_2)]^+$ (**1**) abbreviated as *cis*-$[Cr(CO)_4(dppp)]^+$, (b) *trans*-$[Cr(CO)_2(dppp)_2]^+$ (**2**), and (c) *mer*-$[Cr(CO)_3(\kappa^1\text{-dppp})(\kappa^2\text{-dppp})]^+$ (**3**). Each structure is depicted with the arbitrary molecular frame chosen (M_x, M_y, M_z) and with the **g** tensor principal axes in molecular frame coordinates (g_x, g_y, g_z).

new signal is quite distinct from that of the aforementioned $[Cr(CO)_4(dppp)]^+$ (Figure 1a) or *trans*-$[Cr(CO)_2(dppp)_2]^+$ (Figure 1b,c) complexes discussed earlier. The integrated signal intensity of the low-temperature irradiated spectrum (Figure 1d) decreased with increasing irradiation time, suggesting a progressive loss of the EPR observable Cr(I) in solution. No room-temperature signal could be observed, presumably owing to the fast relaxation behavior of the new complex. A satisfactory simulation of the EPR spectrum (Figure 1d) could only be reproduced by including the addition of two distinct paramagnetic Cr(I) centers into the simulation. The first center was identified as the starting $[Cr(CO)_4(dppp)]^+$ complex (40% spectral contribution after 30 min of irradiation). The second center (60% spectral contribution after 30 min of irradiation) was however different from those observed previously, owing to the presence of two distinct sets of ^{31}P couplings; one arising from a coupling to *two* equivalent phosphorus nuclei (producing the 1:2:1 pattern) with $A_\perp = -50$ to -60 MHz and $A_\parallel = -44$ MHz ($a_{iso} = -51.3$ MHz), and a second coupling arising from the interaction with a *single* phosphorus nucleus (1:1 pattern) characterized by $A_\perp = -70$ to -83 MHz and $A_\parallel = -70$ MHz ($a_{iso} = -74.3$ MHz). It should be recalled that in $[Cr(CO)_4(dppp)]^+$, the two ^{31}P nuclei are equivalent, while in *trans*-$[Cr(CO)_2(dppp)_2]^+$, all four ^{31}P nuclei are equivalent.

The new Cr(I) species responsible for Figure 1d and formed by low-temperature UV irradiation, can be assigned to the *meridional* (*mer*-)$[Cr(CO)_3(\kappa^1\text{-dppp})(\kappa^2\text{-dppp})]^+$ complex (compound **3**, shown in Figure 2c). In this complex, one dppp ligand coordinates in a bidentate mode, while the second ligand coordinates in a monodentate mode. According to DFT, the two magnetically equivalent ^{31}P nuclei arise from one ^{31}P nucleus on the κ^1-dppp ligand and one ^{31}P on the κ^2-dppp bonded ligand, in *trans*- position with respect to each other. The second larger ^{31}P coupling (with $a_{iso} = -74.3$ MHz) then arises from the second ^{31}P nucleus of this κ^2-bonded dppp ligand. One may have expected the two phosphorus nuclei from the κ^2-dppp bonded ligand to be magnetically equivalent, but this does not appear to be the case. The second ^{31}P nucleus on the κ^1-dppp ligand, which is not directly binding to the Cr center, does not show any experimentally observable superhyperfine coupling, confirmed by the DFT A value and almost exactly zero spin density for this phosphorus atom.

This is the first observation of a photochemically formed *mer*-$[Cr(CO)_3(\kappa^1\text{-dppp})(\kappa^2\text{-dppp})]^+$ complex, although previous work demonstrated that the 17-electron *mer*-$[Cr(CO)_3(\kappa^1\text{-L}_2)(\kappa^2\text{-L}_2)]^+$ is the only carbonyl-containing species observed on the electrochemical time scale following electrochemical oxidation of *mer*-$[Cr(CO)_3(\kappa^1\text{-L}_2)(\kappa^2\text{-L}_2)]$.[19−22] The monodentate (κ^1-dppp) ligand may alter its coordination role more readily than the bidentate analogues,[20] and therefore, the choice of backbone linker chain length is expected to be extremely important in determining the thermodynamic and kinetic stability of the 17-electron complexes. It is also known that the *facial* (*fac*-) complexes rapidly isomerize to *meridional* (*mer*-) ones by a thermally activated process,[22] so one would not expect to see the *fac*- complex by EPR.

The EPR spectra obtained upon UV irradiation at 77 K were double integrated, and the values of the 2-fold integrals were plotted vs irradiation time, t_{irr} (Figure 3). In the best-case scenario of the bimolecular reaction going to completion, one

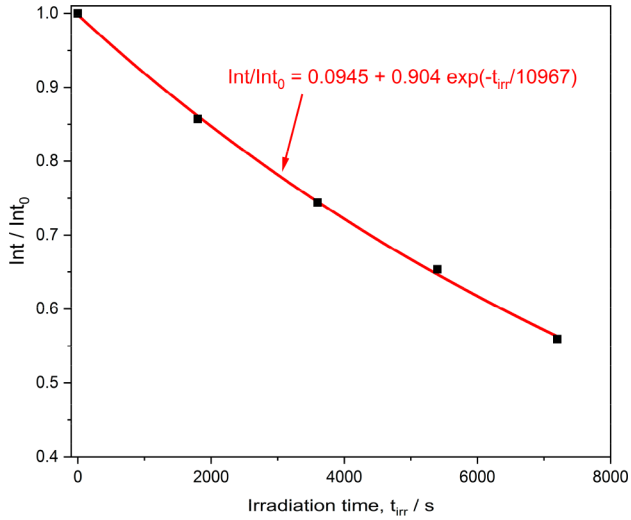

Figure 3. Kinetics of the transformation of starting $[Cr(CO)_4(dppp)]^+$ into *mer*-$[Cr(CO)_3(\kappa^1\text{-dppp})(\kappa^2\text{-dppp})]^+$ following UV irradiation at 77 K.

DOI: 10.1021/acs.organomet.9b00226
Organometallics 2019, 38, 2523−2529

Scheme 2. Proposed Mechanism for Photoinduced Formation of *trans*-$[Cr(CO)_2(dppp)_2]^+$

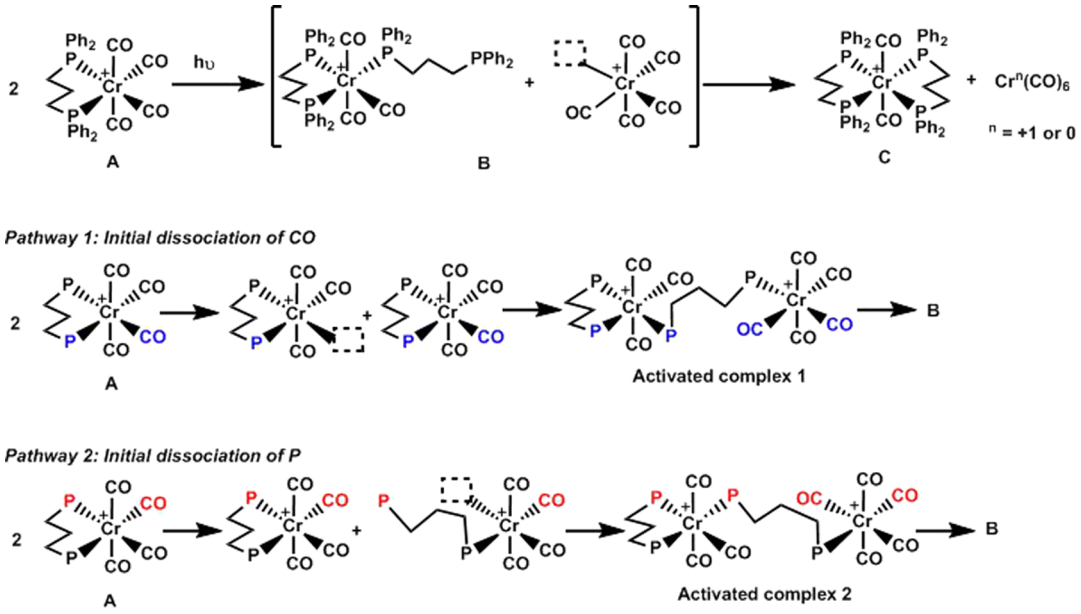

would expect a total loss of spins equal to 50%, if donation of a dppp ligand from one molecule of starting complex to another one results in the former becoming EPR silent (see above). Nevertheless, the trend observed does not asymptotically approach 0.5 but a much lower value, 0.0945. This might indicate that during molecular scrambling leading to the formation of the *mer*- intermediate, the activated complexes of the reaction pathway (Scheme 2) could also lead to the formation of EPR silent byproducts, where disproportionation of two Cr(I) centers might be envisaged, in line with the observations by Rucklidge et al.[16]

Furthermore, in contrast to *trans*-$[Cr(CO)_2(dppp)_2]^+$, the photochemically formed *mer*-$[Cr(CO)_3(\kappa^1\text{-dppp})(\kappa^2\text{-dppp})]^+$ was found to be unstable. When it was allowed to stand in the dark at 298 K for 3 h after irradiation, the mixture of starting and *mer*- complexes revealed the presence of starting $[Cr(CO)_4(dppp)]^+$ complex only, with, as expected, considerably lower signal intensity and depending on the concentration of the starting solution. Previous EPR studies demonstrated the slow transformation of the electrochemically generated *mer*-$[Cr(CO)_3(\kappa^1\text{-dppm})(\kappa^2\text{-dppm})]^+$ into the *trans*-$[Cr(CO)_2\ (dppm)_2]^+$ complex.[18] However, it may be assumed that depending on the solution concentration, it is possible for photochemically generated *mer*-$[Cr(CO)_3(\kappa^1\text{-dppp})(\kappa^2\text{-dppp})]^+$ to transform back to $[Cr(CO)_4\ (dppp)]^+$. Rieger also reported that the formation of the *trans*-Cr(I) complex from the *mer*- complex is a clean and highly efficient process.[17]

In a series of $[Cr^0(CO)_4(L_2)]$ complexes (where L_2 = dppm, dppe, dppp), both the Cr−CO and Cr−P bonds are photolabile.[17] It is therefore not unreasonable to suggest that the same competitive dissociation may be occurring within the Cr(I) complex investigated here. At suitable concentrations, an intramolecular exchange of P and CO ligands could occur (analogous to the $Cr^0(CO)_4$ photochemistry) between neighboring Cr(I) complexes leading to a scrambling of the ligands (Scheme 2). Transient bridged Cr-dppp-Cr dimers can then conceivably form, resulting in the eventual exchange of one dppp ligand from one Cr center to a nearby Cr center, already bearing a κ^2-coordinated dppp ligand. This can then lead to the formation of the EPR visible *mer*-complex. To examine this, the photochemical experiments were repeated on solutions of $[Cr(CO)_4(dppp)]^+$ at three different concentrations. At the highest and lowest concentrations respectively studied here (19.4 and 1.62 mM), no *mer*-$[Cr(CO)_3(\kappa^1\text{-dppp})(\kappa^2\text{-dppp})]^+$ (Figure 1d) or *trans*-$[Cr(CO)_2(dppp)_2]^+$ (Figure 1b,c) complexes were visible in the EPR spectra. At intermediate concentrations (9.7 mM; Figure 1), the *mer*-$[Cr(CO)_3(\kappa^1\text{-dppp})(\kappa^2\text{-dppp})]^+$ and *trans*-$[Cr(CO)_2(dppp)_2]^+$ complexes were readily observed. These results confirm the importance of the concentration-dependent biomolecular mechanisms proposed in Scheme 2. At the highest concentrations (19.4 mM), the intramolecular exchange may reversibly and competitively lead to formation of the starting complex or other EPR silent species, since the overall Cr(I) signal intensity decreased with irradiation time (showing a progressive loss of $[Cr(CO)_4(dppp)]^+$). At the lowest concentrations (1.62 mM), formation of the bridged Cr-dppp-Cr dimers appear to be inhibited, possibly because of an increase of the mean free path, as no *mer*-$[Cr(CO)_3(\kappa^1\text{-dppp})(\kappa^2\text{-dppp})]^+$ complex was found under these conditions.

■ CONCLUSIONS

A combined CW EPR spectroscopy and DFT computational study of a Cr(I)bis(phosphine) complex has been performed to investigate the decarbonylation and phototransformation process of the complex following UV irradiation. Room-temperature irradiation results in the loss of two CO ligands and coordination of an additional dppp phosphine ligand in a bimolecular reaction that produces the stable *trans*-$[Cr(CO)_2(dppp)_2]^+$ complex. On the other hand, low-temperature irradiation (77 K) results in partial loss of CO and formation of the intermediate *mer*-$[Cr(CO)_3(\kappa^1\text{-dppp})(\kappa^2\text{-dppp})]^+$ complex. Upon further UV irradiation at 298 K, this *mer*- species can undergo intramolecular CO displacement to form the stable *trans*-$[Cr(CO)_2(dppp)_2]^+$ complex. The spin Hamiltonian parameters characterizing the *mer*-$[Cr(CO)_3(\kappa^1\text{-dppp})(\kappa^2\text{-dppp})]^+$ and *trans*-$[Cr(CO)_2\ (dppp)_2]^+$ complexes

DOI: 10.1021/acs.organomet.9b00226
Organometallics 2019, 38, 2523−2529

were obtained by simulation of the EPR spectra and confirmed by DFT calculations. The photoinduced formation of the *trans*-$[Cr(CO)_2(dppp)_2]^+$ complex was shown to be concentration-dependent, indicative of a bimolecular mechanism involving two $[Cr(CO)_4(dppp)]^+$ complexes. While these results demonstrate that the $[Cr(CO)_4(dppp)]^+$ complex can undergo facile photoinduced decarbonylation, clear similarities exist with the analogous Cr(0) photochemistry, and this opens up the possibility of generating chromium alkene carbonyl complexes.

EXPERIMENTAL SECTION

All manipulations were performed under a dry and inert atmosphere (N_2 or Ar) using standard Schlenk-line and glovebox techniques. Anhydrous solvents were obtained using an Anhydrous Engineering double alumina column drying system. $CDCl_3$ was degassed and dried over activated molecular sieves (4 Å). 1,3-Bis(diphenylphosphino)-propane (dppp) and silver tetrakis (perfluoro-tert-butoxy)aluminate ($Ag[Al(OC(CF_3)_3)_4]$) were purchased from Sigma and Iolitec, respectively, and used as received. $Cr(CO)_4(dppp)$ and $[Cr(CO)_4(dppp)][Al(OC(CF_3)_3)_4]$ were synthesized according to literature procedures.[5] The ^1H, ^{13}C, and ^{31}P NMR spectra were recorded in $CDCl_3$ on Varian 400-MR or Jeol ECS 400 spectrometers. Chemical shifts (δ) are reported in parts per million (ppm) referenced to the solvent residual peak. Coupling constants (J) are given in Hz and multiplicities abbreviated as br (broad), s (singlet), d (doublet), t (triplet), q (quartet), m (multiplet). Infrared spectra were recorded using a PerkinElmer Spectrum Two FT-IR spectrometer. Mass spectrometry was performed by the University of Bristol mass spectrometry service by electrospray ionization (ESI^+) using a Bruker Daltonics MicroTOF II. For the $Cr(CO)_4(dppp)$ complex the results found were the following: ^1H NMR (400 MHz, $CDCl_3$) δ 7.49−7.30 (m, 20H), 2.42 (dt, J = 9.0, 4.5 Hz, 4H), 1.95 (m, 2H). ^{31}P $\{^1H\}$ (162.0 MHz, $CDCl_3$) δ 42.31 (s). ^{13}C NMR (100.63 MHz, $CDCl_3$) δ 19.79 (CH_2), 30.84 (CH_2), 128.49 (meta-C_6H_5), 129.59 (para-C_6H_5), 131.97 (ortho-C_6H_5), 137.92 (ipso-C_6H_5), 221.82 (cis-CO), 226.21 (trans-CO). Anal. Calcd for $C_{31}H_{26}CrO_4P_2$: C, 64.59; H, 4.55. Found C, 64.78; H, 4.61. IR (CH_2Cl_2) ν_{CO} = 1885 cm^{-1}, ν_{CO} = 1913 cm^{-1} 2005 cm^{-1}. The spectroscopic properties of this compound were consistent with literature data. For the $[Cr(CO)_4(dppp)][Al(OC(CF_3)_3)_4]$, [Cr][Al] system, the results found were the following: ^{19}F NMR (377 MHz, CD_2Cl_2) δ −76.9 (s). ESI_{pos} − MS (DCM): [M + Na] 599.0, [M] 576.0; ESI_{neg} − MS (DCM): [M] 966.9. Anal. Calcd for $C_{47}H_{26}AlCrF_{36}O_8P_2$: C,36.57; H, 1.70. Found C, 36.74; H, 1.74. IR (CH_2Cl_2) ν_{CO} = 1954 cm^{-1}, ν_{CO} = 2046 cm^{-1}, 2086 cm^{-1}. The spectroscopic properties of this compound were consistent with literature data.

Sample Preparation for EPR Measurements. In an nitrogen-filled glovebox, an ampule was loaded with [Cr][Al] (30.0 mg, 0.019 mmol) and DCM (1.00 mL) to give a stock solution 19.4 mM in Cr. Samples were prepared by taking a 200 μL aliquot inside the glovebox and sealing it under an atmosphere of N_2 using a suba-seal. Where dilution was necessary, an aliquot was taken from the stock solution inside the glovebox, and the requisite amount of DCM was added to give a total volume of 200 μL within the EPR tube. The sample was then exposed to UV irradiation for the desired length of time, before the spectrum was recorded. In a number of experiments, additional dppp ligand was also added to the system as follows. In a nitrogen filled glovebox, an ampule was loaded with [Cr][Al] (30.0 mg, 0.019 mmol) and DCM (1.00 mL) to give a stock solution 19.4 mM in Cr. A separate ampule was loaded with dppp (31.8 mg, 0.077 mmol) and DCM (1.00 mL) to give a stock solution 77.0 mM in dppp. The required volumes to give the desired stoichiometries were then added directly to the EPR tube, and the total volume made up to 200 μL by the addition of DCM. The sample was then exposed to UV irradiation for the desired length of time, before the spectrum was recorded. Irradiation was conducted using a Labino Nova Torch UV LED light source with an output power of 112 mW at the sample.

EPR Instrumentation and UV Irradiation. Continuous-wave EPR spectra were recorded on an X-band Bruker EMX spectrometer operating at 100 kHz field modulation frequency, 3 G field modulation amplitude, 10 mW microwave power, and equipped with a high-sensitivity cavity (ER 4119HS). EPR computer simulations were performed using the Easyspin[26] toolbox operating in the Mathworks Matlab environment.

Details of DFT Calculations. On the basis of our previous work,[8−10] the geometry was optimized using Turbomole[27] at the uBP86/def2-TZVP level of theory,[28−30] and confirmed as a true minimum via harmonic frequency calculation. Hyperfine coupling and **g** tensor data was calculated in ORCA[31] PBE0 level of theory,[32] with EPR-II basis set for C and H,[33] def2-TZVP(-f) basis set for P,[30] and the Core Properties (CP) basis set (defined in ORCA for first row transition metals) for Cr.[34]

ASSOCIATED CONTENT

Supporting Information

The Supporting Information is available free of charge on the ACS Publications website at DOI: 10.1021/acs.organomet.9b00226.

Orientations of the **g** and **A** tensors exemplified for the case of the starting $[Cr(CO)_4(dppp)]^+$ (**1**) complex; high-resolution room-temperature spectrum of *trans*-$[Cr(CO)_2(dppp)_2]^+$ (**2**) showing satellite resonances arising from hyperfine coupling to the ^{53}Cr nucleus; and spin Hamiltonian parameters of Cr(I) complexes similar to the ones described in the present work (PDF)

Cartesian coordinates of the *cis*-$[Cr(CO)_4(dppp)]^+$ geometry optimized structure (XYZ)

Cartesian coordinates of the *trans*-$[Cr(CO)_2(dppp)_2]^+$ geometry optimized structure (XYZ)

Cartesian coordinates of the *mer*-$[Cr(CO)_3(\kappa^1\text{-dppp})(\kappa^2\text{-dppp})]^+$ geometry optimized structure (XYZ)

AUTHOR INFORMATION

Corresponding Authors

*E-mail: follia@cardiff.ac.uk.
*E-mail: richardse10@cardiff.ac.uk.
*E-mail: murphydm@cardiff.ac.uk.

ORCID

Stephen L. J. Luckham: 0000-0003-3732-0668
Andrea Folli: 0000-0001-8913-6606
James A. Platts: 0000-0002-1008-6595
Damien M. Murphy: 0000-0002-5941-4879

Notes

The authors declare no competing financial interest.

Information on the data underpinning the results presented here, including how to access them, can be found in the Cardiff University data catalogue at http://doi.org/10.17035/d.2019.0077527126.

ACKNOWLEDGMENTS

EPSRC funding (EP/H023879, EP/P019951) is gratefully acknowledged. S.L.J.L. also acknowledges support from the EPSRC Centre for Doctoral Training in Catalysis (EP/L016443).

REFERENCES

(1) Rucklidge, A. J.; McGuinness, D. S.; Tooze, R. P.; Slawin, A. M. Z.; Pelletier, J. D. A.; Hanton, M. J.; Webb, P. B. Ethylene

DOI: 10.1021/acs.organomet.9b00226
Organometallics 2019, 38, 2523−2529

Tetramerization with Cationic Chromium(I) Complexes. *Organometallics* **2007**, *26*, 2782.
(2) McGuinness, D. S.; Wasserscheid, P.; Keim, W.; Morgan, D.; Dixon, J. T.; Bollmann, A.; Maumela, H.; Hess, F.; Englert, U. First Cr(III)−SNS Complexes and Their Use as Highly Efficient Catalysts for the Trimerization of Ethylene to 1-Hexene. *J. Am. Chem. Soc.* **2003**, *125*, 5272.
(3) Dixon, J. T.; Green, M. J.; Hess, F. M.; Morgan, D. H. Advances in Selective Ethylene Trimerization—A Critical Overview. *J. Organomet. Chem.* **2004**, *689*, 3641−3668.
(4) McGuinness, D. S. Olefin Oligomerization via Metallacycles: Dimerization, Trimerization, Tetramerization, and Beyond. *Chem. Rev.* **2011**, *111*, 2321−2341.
(5) Radcliffe, J. E.; Batsanov, A. S.; Smith, D. M.; Scott, J. A.; Dyer, P. W.; Hanton, M. J. Phosphanyl Methanimine (PCN) Ligands for the Selective Trimerization/Tetramerization of Ethylene with Chromium. *ACS Catal.* **2015**, *5*, 7095−7098.
(6) Skobelev, I. Y.; Panchenko, V. N.; Lyakin, O. Y.; Bryliakov, K. P.; Zakharov, V. A.; Talsi, E. P. In Situ EPR Monitoring of Chromium Species Formed during Cr−Pyrrolyl Ethylene Trimerization Catalyst Formation. *Organometallics* **2010**, *29*, 2943−2950.
(7) Brückner, A.; Jabor, J. K.; McConnell, A. E.; Webb, P. B. Monitoring Structure and Valence State of Chromium Sites during Catalyst Formation and Ethylene Oligomerization by in Situ EPR Spectroscopy. *Organometallics* **2008**, *27*, 3849−3856.
(8) McDyre, L. E.; Hamilton, T.; Murphy, D. M.; Cavell, K. J.; Gabrielli, W. F.; Hanton, M. J.; Smith, D. M. A cw EPR and ENDOR investigation on a series of Cr(I) carbonyl complexes with relevance to alkene oligomerization catalysis: $[Cr(CO)_4L]^+$ (L = $Ph_2PN(R)PPh_2$, $Ph_2P(R)PPh_2$). *Dalton Trans.* **2010**, *39*, 7792−7799.
(9) McDyre, L.; Carter, E.; Cavell, K. J.; Murphy, D. M.; Platts, J. A.; Sampford, K.; Ward, B. D.; Gabrielli, W. F.; Hanton, M. J.; Smith, D. M. Intramolecular Formation of a CrI(bis-arene) Species via TEA Activation of $[Cr(CO)_4(Ph_2P(C_3H_6)PPh_2)]^+$: An EPR and DFT Investigation. *Organometallics* **2011**, *30*, 4505−4508.
(10) Carter, E.; Cavell, K. J.; Gabrielli, W. F.; Hanton, M. J.; Hallett, A. J.; McDyre, L. E.; Platts, J. A.; Smith, D. M.; Murphy, D. M. Formation of $[Cr(CO)_x(Ph_2PN(iPr)PPh_2)]^+$ Structural Isomers by Reaction of Triethylaluminum with a Chromium N,N-Bis(diarylphosphino)amine Complex $[Cr(CO)_4(Ph_2PN(iPr)PPh_2)]^+$: An EPR and DFT Investigation. *Organometallics* **2013**, *32*, 1924−1931.
(11) Mingos, D. M. P. The Electronic Factors Governing the Relative Stabilities of Geometric Isomers of Octahedral Complexes with π-acceptor and π-donor Ligands. *J. Organomet. Chem.* **1979**, *179*, C29−C33.
(12) Compton, R. G.; Barghout, R.; Eklund, J. C.; Fisher, A. C.; Davies, S. G.; Metzler, M. R.; Bond, A. M.; Colton, R.; Walter, J. N. Photoelectrochemistry of some organochromium carbonyl compounds. *J. Chem. Soc., Dalton Trans.* **1993**, 3641−3646.
(13) Szymanska-Buzar, T. Photochemical reactions of Group 6 metal carbonyls with alkenes. *Coord. Chem. Rev.* **2006**, *250*, 976−990.
(14) Gutmann, M.; Jamello, J. M.; Dickebohm, M. S.; Groossekathofer, M.; Lindener-Roenneke, J. Ultrafast Dynamics of Transition Metal Carbonyls: Photodissociation of $Cr(CO)_6$ and $Cr(CO)_6{\cdot}(CH_3OH)_n$ Heteroclusters at 280 nm. *J. Phys. Chem. A* **1998**, *102*, 4138−4147.
(15) Brookhart, M.; Chandler, W.; Kessler, R. J.; Liu, Y.; Pienta, N. J.; Santini, C. C.; Hall, C.; Perutz, R. N.; Timney, J. A. Matrix isolation and transient absorption studies of [bis[bis(pentafluoroethyl)phosphino]ethane]tetracarbonylchromium: intermolecular alkane complexes and intramolecular F-coordination. *J. Am. Chem. Soc.* **1992**, *114*, 3802−3815.
(16) Rucklidge, A. J.; McGuinness, D. S.; Tooze, R. P.; Slawin, A. M. Z.; Pelletier, J. D. A.; Hanton, M. J.; Webb, P. B. Ethylene Tetramerization with Cationic Chromium(I) Complexes. *Organometallics* **2007**, *26*, 2782−2787.
(17) Rieger, A. L.; Rieger, P. H. EPR Study of Photochemical Reactions of *fac*- and *mer*-$[Cr(CO)_3(\eta^1\text{-}L_2)(\eta^2\text{-}L_2)]^+$ (L_2 = Bidentate Phosphine, Arsine, or Phosphonite Ligand). *Organometallics* **2002**, *21*, 5868−5873.
(18) Cummings, D. A.; McMaster, J.; Rieger, A. L.; Rieger, P. H. EPR Spectroscopic and Theoretical Study of Chromium(I) Carbonyl Phosphine and Phosphonite Complexes. *Organometallics* **1997**, *16*, 4362−4368.
(19) Bagchi, R. M.; Bond, A. M.; Colton, R.; Creece, I.; McGregor, K.; Whyte, T. Chemical and Electrochemical Oxidation of *mer*/*fac*-$Cr(CO)_3(\eta^1\text{-L-L})(\eta^2\text{-L-L})$ Containing a Pendant Donor Atom: ESR Studies of the Cations *mer*-$[Cr(CO)_3(\eta^1\text{-L-L})(\eta^2\text{-L-L})]^+$ and trans-$[Cr(CO)_2(\eta^2\text{-L-L})_2]^+$ (L-L = Bidentate Group 15 Ligand). *Organometallics* **1991**, *10*, 2611−2615.
(20) Bond, A. M.; Colton, R.; McGregor, K. Influence of isomeric form, chelated ring size, and the metal on the oxidation of facial and meridional chromium, molybdenum, and tungsten tricarbonyl bis(bis(diphenylphosphino)methane) and bis(1,2-bis(diphenylphosphino)ethane) complexes. *Inorg. Chem.* **1986**, *25*, 2378−2384.
(21) Bond, A. M.; Colton, R.; Jackowski, J. J. Oxidation of chromium, molybdenum, and tungsten dicarbonylbis(diphenylphosphino)methane complexes. *Inorg. Chem.* **1975**, *14*, 2526−2530.
(22) Bond, A. M.; Colton, R.; Jackowski, J. J. Characterization and electrochemical behavior of Group VI dicarbonylbis(diphenylphosphino)methane complexes. *Inorg. Chem.* **1975**, *14*, 274−278.
(23) Rieger, P. H. Electron paramagnetic resonance studies of low-spin d5 transition metal complexes. *Coord. Chem. Rev.* **1994**, *135*−*136*, 203−286.
(24) Bond, A. M.; McGarvey, B. R.; Rieger, A. L.; Rieger, P. H. On the Failure To Observe Isotropic Electron Paramagnetic Resonance Spectra for Certain Chromium(I) Carbonyl Complexes. *Inorg. Chem.* **2000**, *39*, 3428−3429.
(25) Pickett, C. J.; Pletcher, D. Electrochemical synthesis of simple metal carbonyl cations. *J. Chem. Soc., Chem. Commun.* **1974**, *0*, 660−661.
(26) Stoll, S.; Schweiger, A. EasySpin, a comprehensive software package for spectral simulation and analysis in EPR. *J. Magn. Reson.* **2006**, *178*, 42−55.
(27) Ahlrichs, R.; Bar, M.; Haser, M.; Horn, H.; Kolmel, C. Electronic structure calculations on workstation computers: The program system turbomole. *Chem. Phys. Lett.* **1989**, *162*, 165−169.
(28) Becke, A. D. Density-functional exchange-energy approximation with correct asymptotic behaviour. *Phys. Rev. A: At., Mol., Opt. Phys.* **1988**, *38*, 3098.
(29) Perdew, J. P. Density-functional approximation for the correlation energy of the inhomogeneous electron gas. *Phys. Rev. B* **1986**, *33*, 8822R.
(30) Weigend, F.; Ahlrichs, R. Balanced basis sets of split valence, triple zeta valence and quadruple zeta valence quality for H to Rn: Design and assessment of accuracy. *Phys. Chem. Chem. Phys.* **2005**, *7*, 3297−3305.
(31) Neese, F. The ORCA program system. *Wiley Interdiscip. Rev.: Comput. Mol. Sci.* **2012**, *2*, 73−78.
(32) Adamo, C.; Barone, V. Toward reliable density functional methods without adjustable parameters: The PBE0 model. *J. Chem. Phys.* **1999**, *110*, 6158.
(33) Barone, V. in *Recent Advances in Density Functional Methods*, Part I, Ed. Chong, D. P. (World Scientific Publishing Co Pte Ltd, Singapore, 1996).
(34) The ORCA basis set "CoreProp" was used. This basis is based on the TurboMole DZ basis developed by Ahlrichs and coworkers and obtained from the basis set library under ftp.chemie.uni-karlsruhe.de/pub/basen.

DOI: 10.1021/acs.organomet.9b00226
Organometallics 2019, 38, 2523−2529